AAPS PharmSciTech, Vol. 13, No. 4, December 2012 (© 2012)
DOI: 10.1208/s12249-012-9860-x

Research Article

Nanocrystallization by Evaporative Antisolvent Technique for Solubility and Bioavailability Enhancement of Telmisartan

Amrita Bajaj,[1] Monica R. P. Rao,[2,3] Amol Pardeshi,[2] and Dhanesh Sali[2]

Received 17 April 2012; accepted 14 September 2012; published online 28 September 2012

Abstract. Telmisartan is an orally active nonpeptide angiotensin II receptor antagonist used in the management of hypertension. It is a Biopharmaceutics Classification System class II drug having aqueous solubility of 9.9 μg/ml. Telmisartan (TEL) nanocrystals were prepared by evaporative antisolvent precipitation technique using different stabilizers as PVPK30, TPGS, Poloxamer 188, and PEG 6000 in combination or singly. The nanosuspensions were characterized in terms of particle size distribution, zeta potential, and polydispersity index. The suspension containing PVPK30 and TPGS (1:1) showed least average particle size of 82.63 nm and polydispersity index of 0.472. The zeta potential of nanosuspensions ranged between 6.54 and 10.8 mV. An increase of 116.45% was evident in the specific surface area of the freeze-dried product. Contact angle of nanoparticles was also lowered to 27° as compared to 50.8° for TEL. Saturation solubility studies in various media revealed a significant increase in comparison to plain drug. An increase of 3.74× in saturation solubility in FaSSIF and 5.02× in FeSSIF was seen. *In vitro* dissolution profile of nanosuspension coated on pellets revealed release of 85% in water, 95% in 0.1 N HCl, and 75% in phosphate buffer in 30 min. Nanosuspensions were found to be stable in the presence of univalent and bivalent electrolytes. A tenfold increase in bioavailability was evident. Nanoparticles of telmisartan prepared by bottom-up technique proved to be effective in improving the oral bioavailability as a result of enhanced solubility and dissolution rate.

KEY WORDS: biorelevant media; contact angle; specific surface area; telmisartan; TPGS.

INTRODUCTION

Advances in combinatorial chemistry and high throughput screening technologies have revolutionized the process of drug discovery and have led to the development of a large number of molecules with requisite pharmacological activity. However, these immobilized receptor techniques lead to the development of compounds with undesirable physicochemical properties like high lipophilicity, poor aqueous solubility, and high molecular weight (1). Molecules of this type can provide a number of challenges to the formulation scientist and may potentially lead to slow dissolution in biological fluids, insufficient and erratic systemic exposure, and hence sub-optimal efficacy in patients, particularly when delivered by the oral route (2).

There are a number of approaches being used to improve the solubility profile of such drug candidates that include the use of complexing agents such as cyclodextrins; the preparation of high energy drug states related to polymorphic or amorphic transformations; and the use of co-solvents, micellar solutions, and lipid-based systems for lipophilic drugs (3–7). The drawback of these approaches is that the drug should have certain physicochemical properties to make the approach successful, e.g., solubility in oils or the right molecular size to fit into the cyclodextrin ring. The selection of suitable approach is much more difficult for drugs that are poorly soluble in both aqueous as well as organic media thereby excluding all formulation approaches. The number of such drug candidates is steadily increasing, thus necessitating the need for alternative strategies.

A classical approach, based on the Noyes Whitney equation is micronization or nanonization which involves preparing ultrafine powder either in the micron or nanometer size range (8). This facilitates an exponential increase in the interfacial area of contact between the dissolving particles and the dissolution medium thereby enhancing the rate of dissolution of the drug. Top-down methods involve breakdown of coarse particles to the required size range while bottom-up methods involve building particles from solutions by addition of antisolvent. Top-down approaches comprise high-pressure homogenization and media milling which result in the formation of a nanosuspension which can be further dried by spray drying or freeze drying. Bottom-up technology basically involves controlled precipitation by adding a solution of drug to an antisolvent (9). Selection of appropriate solvent combination is very critical to yield a micron or nano-sized product by passing the Ostwald Mier area fast (8). The basic advantage of precipitation technique is its simplicity and use of low-cost equipment.

[1] Department of Pharmaceutics, SVKM'S B.N. College of Pharmacy, Mumbai, India.
[2] Department of Pharmaceutics, AISSMS College of Pharmacy, Kennedy Road, Pune, India.
[3] To whom correspondence should be addressed. (e-mail: monicarp_6@hotmail.com)

Regardless of the technology used for preparing the nanoparticles/crystals, stabilizers such as polymers (steric stabilization) or surfactants (electrostatic stabilization) or a combination of these, are required to ensure that the particles retain their nanosize dimensions. This tendency for the particles to re-agglomerate is due to the increase in the magnitude of interparticulate van der Waals forces of attraction (10).

The aim of the present study was to prepare nanoparticles of telmisartan (TEL) by evaporative antisolvent precipitation technique. TEL is an orally active nonpeptide angiotensin II receptor antagonist that acts on the AT_1 receptor subtype and is used in the management of hypertension. It is a Biopharmaceutics Classification System class II drug having aqueous solubility of 9.9 μg/ml. Its log P and melting point, determined experimentally, were found to be 7.7 and 261–263°C, respectively. TEL has three major functional groups, i.e., methyl benzimidazole, phenyl benzimidazole, and methyl phenyl benzoic acid (Fig. 1) and its pKa is 4.45±0.09. From previous studies in this laboratory, we have found that TEL is poorly soluble in water as well as oils though it is lipophilic in nature. Its high melting point is thus indicative of high crystal energy which reduces its tendency to dissolve in any solvent (11). Such "brick dust" molecules are very brittle and amenable to particle size reduction. However, a drawback of this property is the excessive corrosion of the equipments used for particle size reduction and the associated potential for metal contamination in the product. In this study, we used a combination of bottom-up and top-down technologies to prepare the nanosuspensions of TEL followed by freeze drying to obtain the nanoparticles.

MATERIALS AND METHODS

Materials

TEL was provided by Unichem Laboratories, Mumbai, India as gift sample. Poloxamer 188 and 407 were a gift sample from Signet BASF, Mumbai, India. Talc, polyethylene glycol 6000, and polyvinylpyrrolidone K30 were procured locally from Otto Kemi, Mumbai, India. Acetonitrile, dichloromethane, chloroform, and *N*-methyl pyrrolidone were from Spectrochem Pvt. Ltd., Mumbai, India and were of analytical grade. Tocopheryl polyethylene glycol succinate 1000 was gifted by Isochem, France. Espheres neutral pellets (18–20#) were given as gift by Ideal Cures Pvt. Ltd., Mumbai

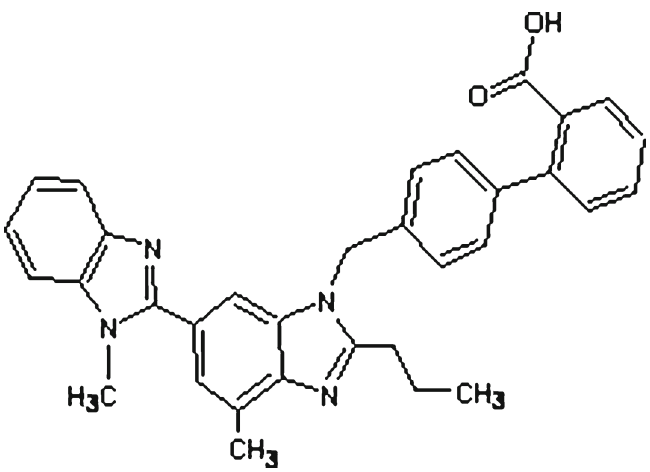

Fig. 1. Structure of TEL

Methods

Determination of Solubility of TEL

The solubility of TEL in water and water miscible or partially water miscible organic solvents such as acetone, acetonitrile, dichloromethane, petroleum ether, chloroform, and *N*-methyl-2-pyrrolidone was determined by adding an excess of the drug in the solvents. Using a magnetic stirrer, the suspensions were stirred for 48 h at 37°C, filtered, and the drug content determined by HPLC. Each sample was analyzed in triplicate.

HPLC Analysis of TEL

The concentration of TEL was determined by RP-HPLC (Agilent Technologies 1120 series, Germany) using TC-C18 column (4.6×250 mm, 5 μm). Acetonitrile and 0.05 M potassium dihydrogen phosphate in a ratio 60:40 (adjusted to pH3.0 with *o*-phosphoric acid) was used as the mobile phase at a flow rate of 1 ml/min. The eluent was analyzed at 271 nm by UV detector. The method was validated for accuracy, precision, and recovery.

Preparation of Nanosuspensions

TEL nanoparticles were prepared by evaporative antisolvent precipitation technique. Preliminary studies were carried out to investigate the solubility of TEL in various solvents like *N*-methyl pyrrolidone (NMP), acetonitrile, dichloromethane, and chloroform. The solvent in which TEL showed highest solubility was used for preparing the nanosuspensions. Required amount of TEL was dissolved in sufficient volume (10 ml) of selected solvent. The polymers/surfactants were dissolved in water (100 ml) separately and the resulting mixture was stirred at 4,000 rpm using a mechanical stirrer (Remi Motor RQT-124A). After formation of a homogenous solution, drug solution was added all at once using a micropipette with continuous stirring. After complete addition of the drug solution, stirring was continued for 2 h at 10,000 rpm. The suspension was kept for some time to allow the foam to dissipate. The different ratios by weight of polymer–surfactant combinations used for preparing nanosuspensions are listed in Table I. Control sample of suspension containing drug alone was prepared using similar conditions as above and subjected to particle size analysis.

Particle Size Measurement

The nanosuspensions were subjected to particle size analysis using Malvern Zetasizer (MAL 500999; Malvern Instruments, UK) based on dynamic light scattering. The measurements were made in triplicate and average particle size, polydispersity index, and zeta potential were determined in deionised and double-distilled water (Merck).

Table I. Formulae for Nanosuspensions of TEL

Sr. No.	Batch code	Components	Ratio
01	T_0	Tel	–
02	T_1	Tel: P188	1:1
03	T_2	Tel: P188: TPGS	1:1:1
04	T_3	Tel: P188: TPGS	1:1:2
05	T_4	Tel: PEG6000	1:1
06	T_5	Tel: PEG6000: TPGS	1:1:1
07	T_6	Tel: PEG6000: TPGS	1:1:2
08	T_7	Tel: PVPK30	1:1
09	T_8	Tel: PVPK30: TPGS	1:1:1
10	T_9	Tel: PVPK30: TPGS	1:1:2

Ultracentrifugation

The nanosuspension which showed maximum decrease in particle size as compared to other nanosuspensions was subjected to ultracentrifugation using Beckmann Coulter (Model: OptimaxXL100K with rotor: SW32Ti) operated at 20,000 rpm and 20°C for 45 min. The residue was subjected to freeze drying at −45°C to −51°C and pressure of 0.08 mbar using LABCONCO Freezone, 2.5, Kansas, USA. The supernatant and freeze-dried products were evaluated for drug content.

Surface Morphology

Morphology of the nanoparticles was investigated by a field emission scanning electron microscope (JSM 6303A, Joel, Tokyo, Japan). The drug particles were sputter coated with gold before observation.

Saturation Solubility

Saturation solubility of plain TEL and freeze-dried nanoparticles was determined by placing excess drug/product in 20 ml deionized water in a capped flask and stirring on an orbital shaker for 48 h. The suspension was double filtered using 0.1 μm filter and the filtrate after suitable dilution was injected into HPLC system and analyzed as previously described. The studies were also conducted in 0.1 N HCl, pH6.8 buffer, and biorelevant media, i.e., FaSSIF and FeSSIF (12).

Fourier Transform Infrared Spectroscopy

The IR spectra was recorded using Fourier transform infrared spectrophotometer (450 plus, Jasco, Japan) with diffuse reflectance principle. The spectrum was scanned over a frequency range of 4,000–400 cm^{-1}. The samples were ground with KBr and pressed into a disk shape for measurement.

Differential Scanning Calorimetry

The differential scanning calorimetry (DSC) thermograms were recorded using differential scanning calorimeter (DSC; 823e, Mettler Toledo, Japan). Approximately 2–5 mg of each sample was heated in a pierced aluminum pan from 30°C to 300°C at a heating rate of 10°C/min under a stream of nitrogen at flow rate of 50 ml/min. Thermal data analyses of the DSC thermograms were conducted using STARe software (version 5.21).

Powder X-ray Diffraction Studies

The powder X-ray diffraction studies (PXRD) spectra of samples were recorded using high power powder X-ray diffractometer (Ru-200B, Pune, India) with Cu as target filter having a voltage/current of 40 KV/40 mA at a scan speed of 4°/min. The samples were analyzed at 2θ angle range of 5–50°. Step time was 0.5 s and time of acquisition was 1 h.

Wettability

Tablets of plain TEL and nanoparticles of TEL were prepared using hydraulic press at pressure of 5 t (model: M-15, Technosearch Instruments, Mumbai) and contact angle between water and tablet surfaces was determined by static sessile drop method (13). It involved placing 10 μl of water on surface of tablet using micropipette. Photographs of the drop were taken after 10 s. It was carefully superimposed on tracing paper and contact angle was measured. Amaranth red was added to water to ensure proper visibility of the drop.

Specific Surface Area

Specific surface area of plain TEL and nanoparticles was measured using BET surface area analyser (model, SAA 2000; make, SP Consultants, Mumbai) using nitrogen as the adsorbate gas at 26°C. The instrument measures the quantity of adsorbate gas desorbed from a solid surface by sensing change in thermal conductivity of a flowing mixture of nitrogen (adsorbate 30%) and helium (inert carrier 70%) gas. The change in thermal conductivity brings about a proportional change in electrical conductivity of the mixture which is measured by the instrument and converted into volume of desorbed gas. The BET equation is used to calculate the specific surface area of the sample as follows:

$$S.A. = \frac{4.38}{W} \times \frac{Sc.Vn}{Nc} \times \frac{273}{(273+t)} \times (1-p/p_0)$$

Where

W Weight of dry/regenerated sample in grams
P Partial pressure of nitrogen in cylinder
p_0 Total partial pressure of gas mixture
t Room temperature in degrees Celcius
Sc Sample counts
Vn Volume of adsorbed gas (N_2) in milliliters

The specific surface area is expressed in meters square per gram of a sample. It is a measure of area covered by nitrogen gas adsorbed in a monolayer form.

Solvent Residue and Metal Contamination

The freeze-dried product was analyzed by gas chromatography for residual solvent and atomic absorption spectroscopy for metal contamination. Shimadzu-GC-2014 system was used with helium as the carrier gas at a temperature range of

50–300°C and pressure of 20 kPa. RTX-Biodiesel TG was used as the column and the detector used was flame ionization detector.

PELLETIZATION OF NANOSUSPENSION

The nanosuspension (T_8) of TEL was spray coated on Espheres (Microcrystalline Cellulose nonpareil seeds 18–20#) using an R & D coating pan (Instacoat, Ideal Cures Pvt.,Ltd., Mumbai). Nanosuspension (80 ml) was sprayed on 20 g of Espheres at 1 ml/min with atomizing air pressure of 2 lb/in. The pan speed was 25 rpm and pellet bed temperature was 60–70°C. Talc was used as an adsorbent to facilitate the drying process.

Dissolution Test

The dissolution test for the nanosuspension coated Espheres was performed in triplicate using USP type I dissolution test apparatus (Electrolab TDT-08 L USP standard). The test was carried out in 900 ml 0.1 N HCl as dissolution medium at 50 rpm and temperature of 37±0.5°C. Aliquots of 5 ml were periodically withdrawn and analyzed. Cumulative percentage of labeled amount of drug released at each time point was calculated. Model fitting was assessed using PCP Disso software.

Pharmacokinetic Studies

In vivo studies were carried out as per the guidelines of the Institutional Animal Ethical Committee (Ref.No.SIOP/IAEC/2011/23). Adult Wistar rats of either sex were used for the study. The rats were weighed, labeled, and divided into three groups; viz. the control group which was administered plain vehicle, the second group which was administered TEL suspension prepared using 1% sodium carboxy methyl cellulose as suspending agent, and the third group which was given TEL nanosuspension. The nanosuspension was prepared by dispersing the freeze-dried nanoparticles in water. They were fasted overnight and water was provided *ad libitum.* The preparations were (4 mg/kg bodyweight) administered to rats using oral feeding tube. The animals were anesthetized with ether before collection of blood which was collected from retro orbital plexus in EDTA-treated tubes. The time intervals for blood withdrawal were of 10 min for the first 30 min followed by 30-min interval for the next 2 h and hourly intervals up to 8 h followed by withdrawal at 12 and 24 h. Plasma was separated by centrifuging the blood at the speed of 3,000 rpm for 10 min at −4°C. The plasma was subjected to protein precipitation by addition of methanol in a ratio of 1:4. It was then centrifuged at 10,000 rpm for 10 min at −4°C. The supernatant was decanted and 20 µl was injected into HPLC column. Simultaneously calibration curve was plotted by spiking known concentration of test drug into the rat plasma and the method was validated over the concentration range of 2–5 µg/ml.

Stability Studies

The nanosuspensions were kept in screw-capped vials at 40°C and 75%RH and under refrigeration (4°C) for a period of 3 months. The effect of monovalent and bivalent electrolytes as well as pH on the physical stability of the nanosuspensions was evaluated by visual observation and measurement of percent transmittance using UV spectrophotometer at 600 nm. For studying the effect of electrolytes, 1 ml of nanosuspension was diluted to 10 ml with deionized water. To this, incremental concentrations (0.5–1.5%) and volume (0.5–2.5 ml) of monovalent (NaCl) were added. In case of bivalent ($CaCl_2$) electrolyte solutions, 0.5–2.5 ml of 0.1–0.5% solutions were added and observed visually after 4 h and 24 h for any changes as well as percent transmission was measured. The stability was also evaluated at pHs 1.2, 4.6, 6.8, and 7.4.

RESULTS AND DISCUSSION

Particle Size Analysis

TEL nanoparticles were prepared by bottom-up technology using evaporative antisolvent precipitation technique. As per the Ostwald–Mier theory (8), crystallization occurs when the solution reaches the appropriate degree of supersaturation which further leads to nucleation and crystal growth. Addition of saturated drug solution to the antisolvent generates a high degree of supersaturation resulting in the formation of large number of nuclei. Supersaturation is facilitated by rapid evaporation of the solvent. This reduces the tendency for crystal growth resulting in the formation of ultrafine crystals. The presence of stabilizers, which undergo preferential adsorption at the surface of particles further arrest the growth of crystals through steric or electrostatic stabilization (14). Additionally, the turbulence created due to high-speed stirring using a robust overhead mechanical stirrer also ensures rapid nucleation and causes breakdown of the crystals thereby preventing them from growing to a larger size. Selection of the right solvent(s) and stabilizer(s) are critical for the nanoprecipitation process. The intention is not only to obtain nanocrystals but also sufficient yield to make the process cost effective. Various solvents that were screened include dichloromethane, chloroform, acetonitrile, and NMP and combinations thereof. Extensive literature was reviewed for selection of various stabilizers commonly used for nanoparticles and then screened for stabilizing TEL nanoparticles. The stabilizers selected included PEG 6000, TPGS, PVP K30, Poloxamer 188 and Poloxamer 407, singly and in combination.

Among the solvents, dichloromethane (DCM/ϵ=8.93) was selected as the solvent for TEL due to its higher solubilization potential for TEL and low boiling point. These two are important parameters as rapid evaporation of the solvent is essential for higher supersaturation and rapid nucleation, all prerequisites for ultrafine crystal size. At the same time, too high a value of dielectric constant (ϵ) will not be beneficial as the drug is highly lipophilic (log P=7.7) and hence it will have limited solubility in the solvent. Though TEL was found to have maximum solubility in NMP its high boiling point (202°C) was a major deterrent as it could have led to problems of solvent residues in the final product. During manufacturing of nanosuspensions, there is an increase in particle surface area due to diminution of particle size and hence an increase in the solid–liquid contact area. This results in an increase in Gibbs free energy thus making the nanosuspensions thermodynamically unstable. An obvious outcome of this would be

Table II. Particle Size Analysis of TEL Nanosuspensions (n=3; Mean±SD)

Sr. No.	Batch code	Zav nm	PDI	$d_{10\%}$	$d_{50\%}$	$d_{90\%}$	ZP (mV)
01	T_0	2,538±10.5	0.499	977	1,410	5,490	6.54±0.98
02	T_1	523.4±21.2	0.685	320	451	642	8.58±1.12
03	T_2	128.2±8.6	0.858	9.77	14.5	35.2	7.88±1.34
04	T_3	591.7±5.5	0.878	603	3,190	5,910	10.8±1.15
05	T_4	778.33±11	0.34	533	772	1,160	9.36±0.96
06	T_5	105.6±3.9	0.440	6.63	18.2	55.0	7.68±0.83
07	T_6	298.2±4.3	0.688	30.4	539	4,560	4.69±0.54
08	T_7	550.67±3.7	1.0	320	451	642	9.38±1.25
09	T_8	82.63±2.8	0.472	10.1	16.2	41.3	7.94±1.38
10	T_9	115.3±4.85	0.481	31.1	48.8	314	8.12±1.11

agglomeration of nanosized particles in an attempt to reduce interfacial area (15). Nanosuspensions were prepared using various polymeric or surfactant stabilizers, singly or in combination and were subjected to particle size analysis and measurement of zeta potential (Table II). It was found that when the stabilizers were used singly the particle size was higher as compared to when they were combined with TPGS (Fig. 2). The average particle size (Zav) of the plain drug suspension prepared under the same conditions was found to be ~2,500 nm. Nanosuspensions containing PVP K30 alone in a ratio of 1:1 showed Zav of 550.6 nm with a PDI of 1.0 whereas with PEG 6000 it was 778 nm with a PDI of 0.34. Nanosuspension containing Poloxamer 188 singly in a ratio of 1:1 with drug showed an average particle size of 523.4 nm. Combining TPGS with the above three polymers in a ratio of 1:1:1 showed a remarkable reduction in particle size thereby confirming the superior stabilizing ability of TPGS. The particle size for these batches ranged from 82.63 to 128.2 nm with the combination of PVPK30 and TPGS showing the least average particle size of 82.63 nm and PDI equivalent to 0.472. The $d_{10\%}$, $d_{50\%}$, and $d_{90\%}$ were found to be 10.1, 16.2, and 41.3, respectively. Poloxamer 188, singly was not effective as a stabilizer, rather flocculation was observed. This could be due to its high hydrophilicity (HLB=29) due to which it may not be undergoing preferential adsorption on the nanocrystal surface. However, in combination with TPGS, it worked synergistically to give a decreased particle size as TPGS has an intermediate HLB of 13. PEG 6000 alone produced nanoparticles with an average size of 778 nm and in combination with TPGS the particle size was found to be approximately 105 nm again alluding to the superior adsorption potential of TPGS and its ability to act synergistically with other surfactants or hydrophilic polymers for stabilizing a nanosystem. Greatest particle size reduction was observed with PVPK30 in combination with TPGS as PVPK 30 is reported to be a protective colloid which is indicative of its greater adsorption potential for the nanoparticles (16). However with all three polymers, an increase in TPGS content led to an increase in particle size which could be attributed to an increase in viscosity due to TPGS (semisolid at room temperature) which precludes the adsorption of stabilizers onto the particles. The zeta potential of all the batches ranged between 6.54 and 10.8 mV. The low values are indicative of the shifting of the plane of shear, at which zeta potential is measured to a larger distance from the particle surface. This is expected as the stabilizers used for preparing the nanosuspensions are either hydrophilic polymers or non-ionic surfactants which stabilize the particles by steric stabilization. Any negative charge might be a result of ionization of surface functional groups present in the drug molecule/stabilizer or adsorption of solvent ions on the particles which gives rise to low zeta potential values.

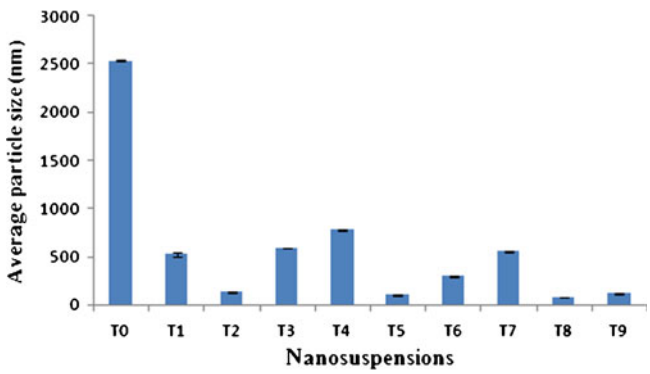

Fig. 2. Average particle size for nanosuspensions T_0–T_9 (nm)

Solid-State Characterization

Batch T_8 containing PVPK30 and TPGS in a ratio of 1:1 was further subjected to characterization since it exhibited the smallest average particle size compared to other batches. The percent yield of nanoparticles was found to be 54% and drug content was found to be 7.649 /10 mg of product. The specific surface area of T_8 was found to be 8.327 m^2/g whereas for TEL it was 3.847 m^2/g, i.e., an increase of 116.45% was evident (Fig. 3). Increase in specific surface area corroborates the

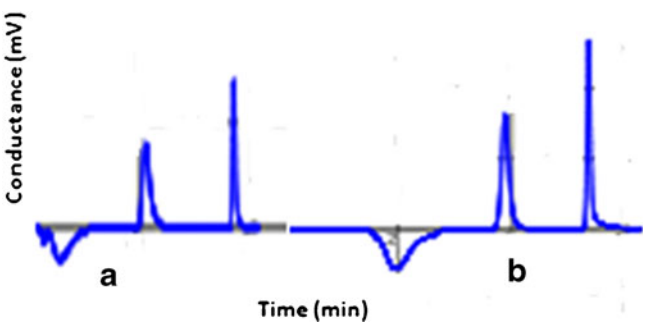

Fig. 3. Specific surface area of **a** plain TEL **b** NC

Fig. 4. Contact angle of **a** plain TEL **b** NC

decrease in particle size and therefore providing increased interfacial area of contact with the dissolution medium. A drawback of nanosized particles could be the increase in solid–liquid interfacial tension which could adversely impact the wettability. However, the presence of hydrophilic polymers and surfactants adsorbed at the interface tend to reduce the interfacial tension. This is confirmed by contact angle measurements (Fig. 4) which for the pure drug was found to be 50.8° (n=3) and for the nanoparticles it was 27° (n=3). Lower contact angle is indicative of improved wettability of the nanoparticles.

The SEM micrographs revealed rod-shaped crystals of TEL with rounded (blunt) edges and smooth surface (Fig. 5a and b). Plain drug is highly crystalline showing sharp needle-shaped crystals. The PXRD spectra of the nanoparticles are a replica of the plain drug indicating that there was no perceptible change in the crystallinity of the TEL (Fig. 6a and b). The gas chromatogram revealed absence of solvent peak. Though DCM is highly volatile (boiling point=40°C), this test was performed to rule out the possibility of solvent molecules entrapped within the nanocrystal structure. It has been reported that solids having high melting point have stronger crystal lattice energy and are brittle/hard in nature and hence greater particle size reduction is possible (11). At the same time, chances of metallic contamination due to erosion increases. Since the processing involved stirring at 10,000 rpm for 2 h and TEL being a highly crystalline solid, the nanosuspension was screened for metal content, i.e., Fe and Cr by atomic absorption spectroscopy. The iron content was found to be <2 ppm and chromium was <0.1 ppm.

The compatibility of TEL with the selected stabilizers was investigated using DSC (Fig. 7). Binary physical mixtures of the drug with stabilizers (1:1) were subjected to thermal analysis. There was no evidence of incompatibility in the mixtures. TEL showed a sharp melting endotherm with an onset at 267.31°C, peak at 269.22°, and endset at 271.88° indicating its purity and crystallinity. The enthalpy was found to be 479.98 mJ. The thermogram of the nanoparticles revealed an endotherm with an onset temperature of 265.68°, peak at 268.55°, and endset at 272.19°C. However, the peak height

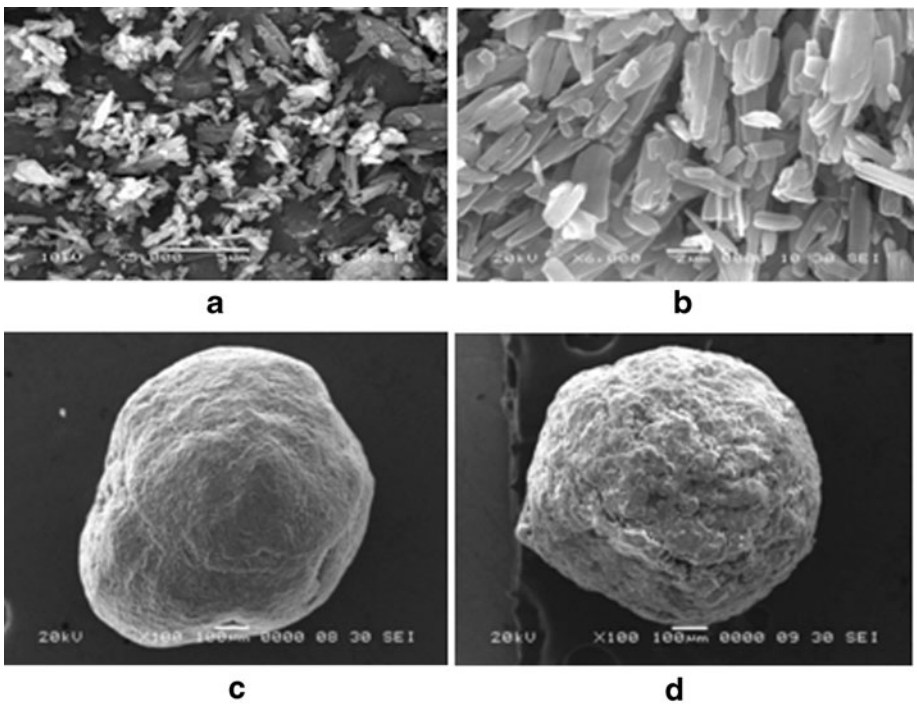

Fig. 5. SEM of **a** TEL, **b** NC, **c** plain Espheres, **d** nanosuspension-coated Espheres

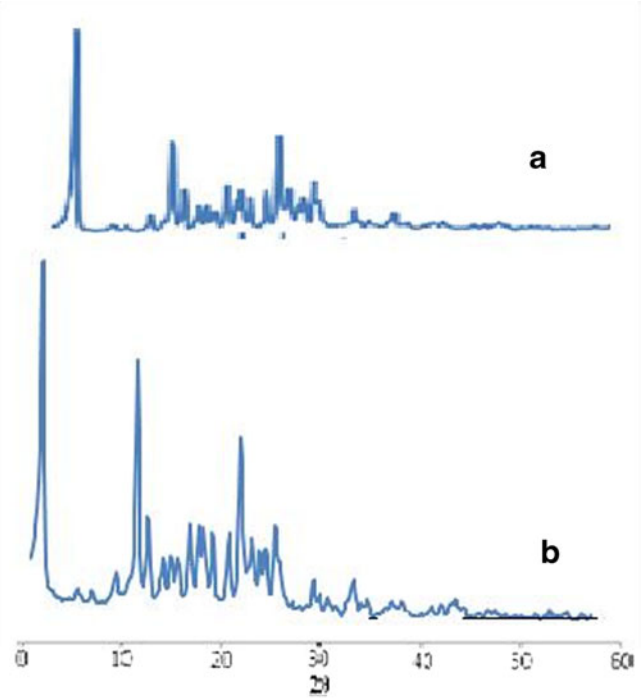

Fig. 6. PXRD spectra of **a** TEL, **b** NC

was considerably reduced and the enthalpy was found to be 396.79 mJ which could be attributed to dilution effect of the stabilizers present in the nanoparticles.

Saturation Solubility

Saturation solubility studies in various media revealed an exponential increase in comparison to plain drug (Fig. 8). The solubility of nanoparticles in 0.1 N HCl was found to be 156.1 μg/ml, an almost 4.3-fold increase. In distilled water, the increase was 16-fold; in phosphate buffer pH6.8, the increase was to the tune of sixfold. When dissolution testing is used to forecast the *in vivo* performance of a drug, it is critical that the *in vitro* test mimic the conditions *in vivo* as closely as possible. Biorelevant media, i.e., FaSSIF and FeSSIF help to simulate *in vivo* conditions and can be used as barometers for predicting *in vivo* changes in solubility pattern especially for poorly soluble drugs. TEL itself showed higher saturation solubility in the two media. However, the nanoparticles showed an exponential 3.74× increase in solubility in FaSSIF and 5.02× in FeSSIF.

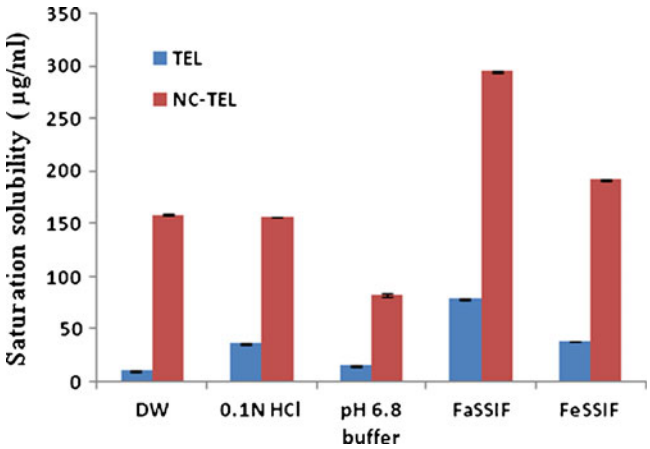

Fig. 8. Saturation solubility in different media; *blue* TEL, *red–orange* NC

Results in biorelevant media indicate the absence of crystal growth phenomena or particle agglomeration when exposed to GI fluids. Formation of mixed micellar systems due to presence of soya lecithin and sodium taurocholate in biorelevant media could be synergistically involved with particle size reduction in improving solubility of TEL. Thus, the true predictors for success of a solubility enhancing technology are the studies carried out in biorelevant media. For drugs like TEL, which show pH dependent solubility, the difference in solubility in FaSSIF and FeSSIF could have an important consequence on the *in vivo* absorption pattern and thus can aid in the design of drug delivery systems for a drug. The overall increase in saturation solubility in all media could be attributed to the increased dissolution pressure which is described by the Ostwald–Freundlich equation (17) which correlates particle size with the saturation solubility and states that with decreasing particle size the dissolution pressure increases thereby increasing the saturation solubility of the solute.

In Vitro Dissolution

The *in vitro* dissolution studies in water revealed a significant improvement in the dissolution efficiency with 98% drug being dissolved in 20 min whereas for pure drug (T_0) 3.9% was released in 100 min. In 0.1 N HCl 99% drug was released in 20 min in case of nanoparticles whereas for TEL 40% release was observed in the same time frame. In phosphate buffer pH6.8 almost 99% drug was released in 60 min as against <5% for TEL. The Qt_{30min} is depicted in Fig. 9.

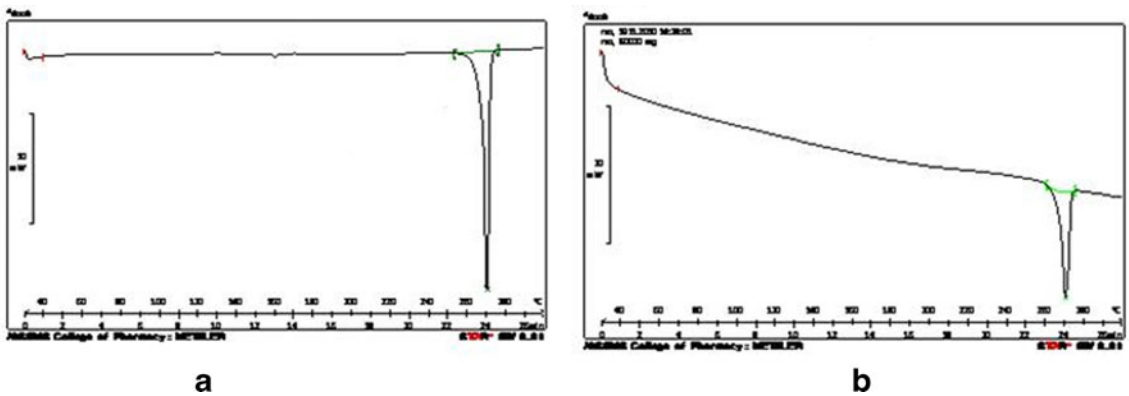

Fig. 7. DSC thermograms of **a** TEL, **b** NC

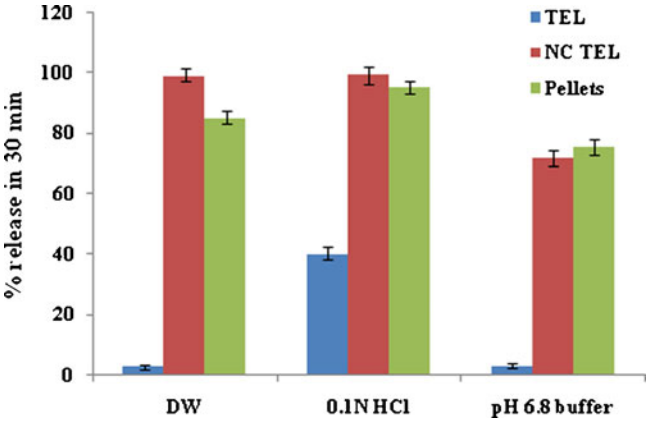

Fig. 9. Qt_{30min} for TEL, NC and pellets; *blue* TEL, *red–orange* NC, *yellow green* pellets

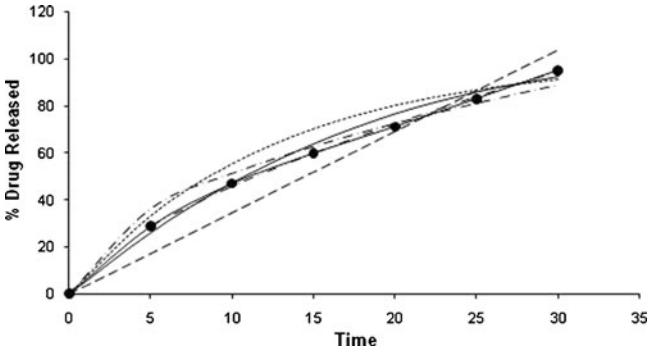

Fig. 10. *In vitro* dissolution profile of TEL nanosuspension spray-coated Espheres; *line with black circle* actual, *dash line* zero, *dotted line* first, *dash–dot line* matrix, *dash-double dot line* Peppas, solid line Hixon Crowell

According to the Prandtl equation, the diffusional distance "*h*" is reduced for small particles. The simultaneous increase in saturation solubility and decrease in "*h*" leads to an increased concentration gradient, thus enhancing the dissolution velocity (18).

$$h_H = k.L^{1/2}/V^{1/2} \quad (1)$$

h_H hydrodynamic boundary layer thickness
k constant
L length of surface in direction of flow
V relative velocity of flowing liquid *vs* flat surface

The higher curvature of smaller particles results in a reduced surface in the direction of flow.

Dissolution Studies on Spray-Coated Espheres

The *in vitro* dissolution profile revealed that almost 95% drug was released in 30 min in 0.1 N HCl from the spray coated Espheres. Model fitting using PCP Disso software revealed that the release followed Peppas model as evident from the regression coefficient and the dissolution constant (Table III, Fig. 10). The percent release in water was 85% and in phosphate buffer, it was 75% release in 30 min. The SEM of the uncoated Espheres display a smooth surface whereas the coated Espheres show the nanoparticles embedded on the surface (Fig. 5c and d).

Table III. Dissolution Constants for TEL Nanosuspension (T_8) in Distilled Water (n=3) (Mean ± SD)

Model	*R*	*k*
Zero order	0.9655	3.4677
T test	8.297	(Passes)
First order	0.9413	−0.0809
T test	6.235	(Passes)
Matrix	0.9899	16.2325
T test	15.649	(Passes)
Peppas	0.9995	10.1144
T test	67.911	(Passes)
Hixon Crowell	0.9860	−0.0192
T test	13.210	(Passes)

Stability Studies

The nanosuspension (T_8), subjected to different environmental conditions were visually observed for any physical changes. Besides this, particle size distribution was also determined. Effect of different pHs, monovalent and bivalent electrolytes was investigated. TEL itself is an unusually stable molecule and did not undergo any decomposition in any climatic condition (19). The Zav of nanosuspension kept under ambient conditions was found to be 246.8 nm with a polydispersity of 0.578. An increase of 1.98-fold in average particle size was evident compared to 82.63 nm. In case of samples of T_8 nanosuspension kept at 40°C/75%RH and under refrigeration the Zav was found to be 332.5 and 322.5 nm, respectively. The $d_{10\%}$, $d_{50\%}$, and $d_{90\%}$ were found to be 112, 196, and 232.3 nm for samples kept under ambient conditions while the same for T_8 nanosuspension kept at 40°C/75%RH were 125.5, 258.6, and 312 nm and for samples kept under refrigeration, the $d_{10\%}$, $d_{50\%}$, and $d_{90\%}$ were found to be 136, 288.3, and 315 nm, respectively. The polydispersity was found to be 0.277 and 0.267, respectively. The marginal increase in particle size could be attributed to Ostwald ripening. However, the particles still retained an acceptable size in the nanometer range. To evaluate *in vivo* robustness of the nanosuspension pH was adjusted to 1.2, 4.6, 6.8, and 7.4 by addition of either 1% acetic acid or 1% sodium hydroxide solution and percent transmittance was measured. A decrease would be indicative of flocculation or increase in particle size. There was no apparent change in the percent transmittance (Table IV) at various pHs indicating stability of the formulation in the dynamic pH conditions existing in the gastrointesnal tract (GIT). No

Table IV. Percent Transmittance of TEL Nanosuspension (T_8) at Various pHs (n=3; mean±SD)

Sr. No	pH	% transmittance
01	1.2	48.63±2.24
02	4.6	46.65±1.40
03	6.8	44.89±2.17
04	7.4	43.84±1.85

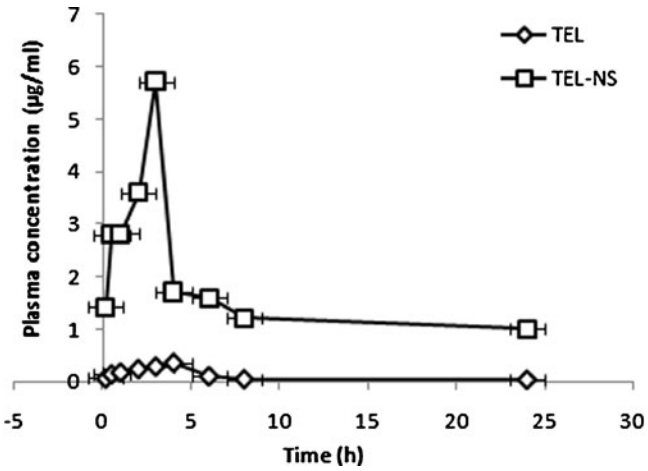

Fig. 11. Plasma concentration–time profile for TEL and TEL nanosuspension (mean±SEM)

flocculation or sedimentation was evident even after 5 days. Colloidal and subcolloidal particles are susceptible to agglomeration in presence of electrolytes as they are capable of disrupting the barrier layer (especially electrostatic barrier) surrounding the particles. Bivalent ions are stronger destabilizers than monovalent ions as per the Schulze–Hardy rule (20). The problem is particularly manifest in nanoparticles that are electrostatically stabilized. Though the present study involved steric stabilization, the authors intended to investigate any interaction between the electrolytes and the polymers/surfactants used for stabilizing the nanosuspension. No significant change in the percent transmittance of the nanosuspensions (T_8) measured before and after addition of incremental volumes and concentrations of both NaCl and $CaCl_2$ was seen. This is indicative of the resilience of the polymeric/surfactant interfacial barrier towards destabilization in presence of electrolytes.

Pharmacokinetic Studies

The area under curve (AUC) is an important pharmacokinetic parameter to corelate exposure time of drug with pharmacodynamic activity and formulations which are long circulating are expected to show higher AUC values (21). Noncompartmental analysis is carried out to compute the pharmacokinetic parameters. The plasma concentration–time profile for plain TEL and TEL nanosuspension is depicted in Fig. 11. A significant improvement in bioavailability is evident form the graph. The AUC was calculated using the trapezoidal rule and is reported in Table V. Area first moment curve (AUMC) was obtained from the plot of product of plasma drug concentration and time *vs* time. A 10.6-fold increase in $AUC_{0–24}$ is indicative of significant enhancement in bioavailability of TEL in the form of nanosuspension. The AUMC was found to be 37.362 and 685.341 for plain TEL and the TEL nanosuspension, respectively. The mean residence time was calculated as 10.43 h for TEL and 18.04 h for TEL nanosuspension. Thus, an increase of 1.72 times was evident in the MRT for the prepared nanosuspension. The apparent elimination rate constant computed from the reciprocal of MRT was found to be 0.095 h^{-1} for TEL and 0.055 h^{-1} for the nanosuspension. This corroborates the MRT values of the formulations. The $t_{1/2}$ was found to be 10.12 and 29.5 h, respectively, for TEL and TEL nanosuspension. A 15.6-fold increase in C_{max} was observed from 0.364 µg/ml for TEL to 5.7 µg/ml for the nanosuspension. The use of particle size reduction to increase the surface area for dissolution and thereby increase bioavailability of poorly water-soluble drugs has been widely investigated and accepted worldwide. Decreasing particle size increases the surface-to-volume ratio and specific surface area (22). Agglomeration in the GIT, resulting in a decrease in the effective surface area, is a major problem for submicron particles in necessitating the use of stabilizers (23). The tenfold increase in $AUC_{0–24}$ of TEL nanosuspension could be attributed to the greater dissolution rate of TEL nanoparticles owing to reduced particle size with increased surface area and reduced diffusion layer thickness. The presence of PVPK 30 and TPGS as stabilizers precludes the agglomeration of nanoparticles in the GIT and improves wettability thus facilitating the dissolution process. Besides this, particles size has been recognized as a crucial parameter for bioadhesion to and absorption from gastrointestinal tissue (24). The dissolution profiles showed that the drug nanosuspension had the highest dissolution rate as compared to plain drug. Hence, they could dissolve easily into intestinal fluid and smaller particles show a higher extent of uptake than larger ones via both follicle associated epithelia and absorptive enterocytes (25). The nearly 1.72-fold increase in MRT and decrease in elimination rate constant for the nanosuspension as compared to plain TEL also supports the AUC data.

CONCLUSION

Nanosizing was a classical approach to enhance solubility and dissolution velocity of poorly water-soluble drugs. Bottom-up technology is a simple and cost effective approach for producing nanoparticles. It is not an energy-intensive process like top-down technology which may bring about pharmaceutically detrimental changes in the crystalline form of the drug. The drawback of solvent residue can be tackled by use of highly volatile solvents in limited quantities. Multitude approaches are available to convert the nanosuspensions into solid dosage forms to improve handling properties. In the present work, the nanosuspension was further converted into solid dosage form by layering onto nonpareil seeds. Nanosizing was successfully applied to improve the saturation solubility, dissolution rate and bioavailability of telmisartan.

Table V. Pharmacokinetic Parameters for Nanosuspension (T_8, n=3; mean±SEM)

	$AUC_{0–24}$	$AUMC_{0–24}$	MRT (h)	C_{max} (µg/ml)	T_{max} (h)
TEL	3.5813±0.04	37.362±0.08	10.43±0.06	0.364±0.06	4±0.05
TEL nanosuspension	37.97±0.089	685.341±0.04	18.04±0.056	5.7±0.078	3±0.06

ACKNOWLEDGEMENTS

The authors would like to acknowledge Dr. Jay Kannan (IISER, Pune), Mr. Tamhane (SP Consultants, Mumbai), Dr. RA Joshi (NCL, Pune) and Dr. Shouche (NCCS, Pune) for their help in the study.

REFERENCES

1. Vandecruys R, Peeters J, Verreck G, Brewster M. Use of screening method to determine excipients which optimize the extent and stability of supersaturated drug solutions and application of this system to solid formulation design. Int J Pharm. 2007;342:168–75.
2. Blagden N, de Matas M, Gavan PT, York P. Crystal engineering of active pharmaceutical ingredients to improve solubility and dissolution rates. Adv Drug Del Rev. 2007;59:617–30.
3. Kim C, Park J. Solubility enhancement for oral delivery: can chemical structure modification be avoided? Am J Drug Deliv. 2004;2:113–30.
4. Merisko-Liversidge E, Liversidge G, Cooper E. Nanosizing: a formulation approach for poorly water soluble compounds. Eur J Pharm Sci. 2003;18:113–20.
5. Humberstone A, Charman W. Lipid-based vehicles for the oral delivery of poorly water soluble drugs. Adv Drug Del Rev. 1997;25:103–28.
6. Forster A, Rades T, Hempenstall J. Selection of suitable drug and excipient candidates to prepare glass solutions by melt extrusion for immediate release oral formulations. Pharm Tech Eur. 2002;14:27–37.
7. Davis ME, Brewster ME. Cyclodextrin-based pharmaceutics: past, present, future. Rev Drug Discov. 2004;3:1023–35.
8. Keck C, Muller R. Drug nanoparticles of poorly soluble drugs produced by high pressure homogenization. Eur J Pharm Biopharm. 2006;62:3–16.
9. Timpe C. Oral drug solubilization strategies: applying nanoparticulate formulation and solid dispersion approaches in drug development. Featured Article in APV Drug Delivery Focus Group Newsletter. 2010:1.
10. Huang P, Wang X, Chen Z. Micronization of gemfibrozil by reactive precipitation process. Int J Pharm. 2008;360:58–64.
11. Kocbeck P, Baumgartner S, Kristl J. Preparation and evaluation of nanosuspensions for enhancing the dissolution of poorly soluble drugs. Int J Pharm. 2006;312:179–86.
12. Dressman J, Amidon GL, Reppas C, Shah V. Dissolution testing as a prognostic tool for oral drug. Absorption: immediate release dosage forms. Pharm Res. 1988;15:11–22.
13. http://en.wikipedia.org/wiki/Sessile_drop_technique. Accessed on 6 Dec 2011
14. Matteucci M, Hotze M, Johnston K, Williams R. Drug nanoparticles by antisolvent precipitation:mixing energy *vs* surfactant stabilization. Langmuir. 2006;22:8951–9.
15. van Eerdenbrugh B, Froyen L, van Humbeeck J, Martens J, Augustijns P, van den Mooter G. Top-down production of drug nanoparticles: nanosuspension stabilization, miniaturization and transformation into solid products. Int J Pharm. 2008;364:64–75.
16. http://www.greatvistachemicals.com/industrial&specialtychemicals/polyvinylpyrrolidone.html. Accessed on 10 Nov 2011
17. Born P, Klaessig FC, Landry TD, Moudgil M, Pauluhn J, Thomas K, Trottier R, Wood S. Research strategies for safety evaluation of nanomaterials, part V: role of dissolution in biological fate and effects of nanoscale particles. Toxicol Sci. 2006;90(1):23–32.
18. Bisrat M, Anderberg EK, Barnett MI, Nyström C. Physicochemical aspects of drug release XV. Investigation of diffusional transport in dissolution of suspended, sparingly soluble drugs. Int J Pharm. 1992;80:191–201.
19. Weinen W, Entzeroth M, Jacobus C. A review on Telmisartan: a novel, long-acting angiotensin II-receptor antagonist. Cardiovascular Drug Reviews. 2000;18(2):127–54.
20. Sinko Patrick J. Martin's physical pharmacy and pharmaceutical sciences. 5th ed. Philadelphia: Lippincott Williams & Williams; 2006. p. 486.
21. Panchagnula R, Dhanikula A, Singh R. *In vivo* pharmacokinetic and tissue distribution studies in mice of alternative formulations for local and systemic delivery of paclitaxel: gel, film, prodrug, liposomes and micelles. Curr Drug Del. 2005;2:35–44.
22. Liversidge GG, Conzentino P. Drug particle size reduction for decreasing gastric irritancy and enhancing absorption of naproxen in rats. Int J Pharm. 1995;125:309–13.
23. Higuchi W, Swarbick J, Ho N, Simonelli AP, Martin A. In: Gennaro AR, editor. Remington's pharmaceutical sciences. Easton: Mack; 1985. p. 301–29.
24. Wei L, Yonggang Y, Yongshou T. Preparation and *in vitro*/*in vivo* evaluation of revaprazan hydrochloride. Int J Pharm. 2011;408:157–62.
25. Jani P, Halbert G, Langridge J, Florence AT. Nanoparticle uptake by the rat gastrointestinal mucosa: quantitation and particle size dependency. J Pharm Pharmacol. 1990;42:821–6.